Journal of Photochemistry and Photobiology A: Chemistry 208 (2009) 110–116

Contents lists available at ScienceDirect

Journal of Photochemistry and Photobiology A: Chemistry

journal homepage: www.elsevier.com/locate/jphotochem

Synthesis and photoluminescent properties of five homodinuclear lanthanide (Ln^{3+} = Eu^{3+}, Sm^{3+}, Er^{3+}, Yb^{3+}, Pr^{3+}) complexes

Hong-Yan Li[a], Jing Wu[a], Wei Huang[a], Yong-Hui Zhou[a], Huan-Rong Li[b], You-Xuan Zheng[a,*], Jing-Lin Zuo[a,*]

[a] State Key Laboratory of Coordination Chemistry, Nanjing National Laboratory of Microstructures, School of Chemistry and Chemical Engineering, Nanjing University, Nanjing 210093, PR China
[b] School of Chemical Engineering, Hebei University of Technology, Tianjin 300130, PR China

ARTICLE INFO

Article history:
Received 9 June 2009
Received in revised form 17 August 2009
Accepted 3 September 2009
Available online 8 September 2009

Keywords:
Homodinuclear lanthanide complexes
2,2′-Bipyrimidine
Photoluminescence
Characteristic luminescence
Quantum efficiency

ABSTRACT

A series of homodinuclear lanthanide complexes $Ln_2(HTH)_6Bpm$ (where Ln = Eu, Sm, Er, Yb, Pr; HTH = 4,4,5,5,6,6,6-heptafluroro-1-(2-thienyl)hexane-1,3-dione; Bpm = 2,2′-bipyrimidine) were synthesized and the photoluminescence properties of these complexes are described. After ligand-mediated excitation of the complexes, they all show the characteristic luminescence of the corresponding Ln^{3+} ions in the visible and NIR regions attributed to efficient energy transfer from the ligands to the metal centres. For the $Eu_2(HTH)_6Bpm$ complex a lifetime of 738.8 μs (100%, χ^2 = 1.362) is found in solid and two lifetimes of 455.4 μs (12.88%) and 618.5 μs (87.12%) (χ^2 = 1.652) are found in CH_2Cl_2 solution, respectively. Its quantum efficiency in air-equilibrated CH_2Cl_2 solution is found to be 28.4%, by using air-equilibrated aqueous $[Ru(bpy)_3]^{2+}\cdot 2Cl^-$ solution as reference sample (Φ_{std} = 2.8%).

1. Introduction

There are two main advantages for using lanthanide complexes in organic light-emitting diodes (OLEDs) [1], sensors [2], molecular optoelectronic devices [3,4], etc. One is the very sharp emission of lanthanide ions from electronic transitions within the 4f subshells due to the effective shielding by the overlying 5s and 5p orbitals. Another is the possibility of increasing the quantum efficiency as high as 100% in theory caused by the intramolecular energy transfer that consists of the absorption of energy by organic ligands, intersystem crossing into a triplet state of the organic ligands, and energy transfer to the central lanthanide cation [5–9]. A number of mononuclear lanthanide complexes including visible and near-infrared-emitting ones have been applied in the electroluminescent (EL) studies and other fields [5–14]. At the same time, the exploration of dinuclear lanthanide complexes is receiving considerable attention. Several groups such as Wang and co-workers [15,16], Shim and co-workers [17], Eliseeva et al. [18,19], Legendziewicz et al. [20], and Swavey and co-workers [21–23] reported the synthesis and luminescence properties of dimeric lanthanide β-diketonates. It is necessary to synthesize and investigate more dinuclear lanthanide complexes with different molecular structures, both in visible and near-infrared regions, to understand the luminescence mechanism and find good materials.

In addition, recently, considerable attention has been paid to the near-infrared (NIR) luminescence of trivalent lanthanide ions because the lanthanide ions have potential applications in the telecommunication network optical signal amplifier [24,25], and diagnostic values as luminescence probes [26]. For example, the Yb^{3+} ion emission occurs in the NIR region (approximately 1000 nm) where biological tissues and fluids (e.g., blood) are relatively transparent, thus the development of Yb^{3+} ion luminescence for various analytical and chemosensor applications is promising. Nd-containing systems have been regarded as the most popular infrared luminescent materials for application in laser systems (the basis of the common 1064-nm laser). Two telecommunication windows for amplification are commonly used for long-distance communication, one at 1.3 μm using Nd emission and the other at 1.5 μm using Er or Ho emission [27–30].

In this paper, we describe the synthesis of a series of homodinuclear lanthanide complexes based on Bpm (2,2′-bipyrimidine) as bridging ligand and HTH (4,4,5,5,6,6,6-heptafluroro-1-(2-thienyl)hexane-1,3-dione) as the sensitizing ligand. Bpm is a planar heterocycle capable of coordinating to two metal centers through equivalent nitrogen atoms. This bonding motif has been exploited in the synthesis of numerous bimetallic transition metal complexes [31,32]. HTH can sensitize several lanthanide ions efficiently due to the suitable triplet energy level and the low C–F vibration energy [33,34].

* Corresponding authors. Tel.: +86 25 83596775; fax: +86 25 83314502.
E-mail address: yxzheng@nju.edu.cn (Y.-X. Zheng).

1010-6030/$ – see front matter © 2009 Elsevier B.V. All rights reserved.
doi:10.1016/j.jphotochem.2009.09.003

2. Experimental

2.1. Materials and instrumentation

Lanthanide chloride hexahydrates ($LnCl_3{\cdot}6H_2O$, Ln = Eu, Sm, Er, Yb, Pr) were purchased from Ruike Co. (China). HTH was obtained from Aldrich (USA). 2-Bromopyrimidine was bought from JinTan Hunter Chemical Co. (China). Elemental analyses for C, H, and N were performed on a PerkinElmer 240C analyzer. Fluorescence spectra in visible region were measured with a Hitachi F4600 luminescence spectrophotometer. The photoluminescence lifetime and fluorescence spectra in IR region measurements were measured with an Edinburgh Instruments FLS920P fluorescence spectrometer. Thermogravimetrical analysis (TGA) was performed in N_2 atmosphere with a flow rate of 100 mL/min on a simultaneous SDT 2960 thermal analyzer from 20 °C to 750 °C, with a ramp rate of 10 °C/min. The crystal of $Eu_2(HTH)_6Bpm$ suitable for single-crystal X-ray analysis was obtained by slow evaporation of an acetonitrile solution. The data were collected on a Bruker Smart Apex CCD diffractometer equipped with Mo Kα (λ = 0.71030 Å) radiation at 293 K. The data reduction SAINT program and absorption corrections were applied using SADABS supplied by Bruker. The structure was solved by direct methods and refined by full-matrix least-squares methods on F^2 using SHELXTL-97.

We used two methods to calculate the quantum yield of the lanthanide complexes luminescence. The quantum yield of the luminescence, Φ, expresses how well the radiative processes (characterized by rate constant, k_r) compete with non-radiative processes (overall rate constant, k_{nr}), may be defined as Eq. (1):

$$\Phi = \frac{k_r}{k_r + k_{nr}} \quad (1)$$

Non-radiative processes influence the observed luminescence lifetime ($\tau_{obs} = (k_r + k_{nr})^{-1}$). The radiative (or natural) lifetime, which—by definition [35]—is not affected by these processes ($\tau_R = k_r^{-1}$). So, if the radiative lifetime, τ_R, is known, Φ can be calculated using the observed luminescence lifetime τ_{obs} (Eq. (2)) [36]:

$$\Phi = \frac{\tau_{obs}}{\tau_R} \quad (2)$$

The popular method to calculate the luminescence quantum yield is to compare the fluorescence intensities (integrated areas) of a standard sample (air-equilibrated aqueous $[Ru(bpy)_3]^{2+}{\cdot}2Cl^-$ solution, $\Phi_{std} = 2.8\%$) and the unknown sample according to Eq. (3) [37]:

$$\Phi_s = \Phi_{std}\left(\frac{I_s}{I_{std}}\right)\left(\frac{A_{std}}{A_s}\right)\left(\frac{\eta_s}{\eta_{std}}\right)^2 \quad (3)$$

where Φ_s is the luminescence quantum yield of the unknown sample, Φ_{std} is the luminescence quantum yield of the standard air-equilibrated aqueous $[Ru(bpy)_3]^{2+}{\cdot}2Cl^-$ solution, I_s and I_{std} are the integrated fluorescence intensities of the unknown sample and $[Ru(bpy)_3]^{2+}{\cdot}2Cl^-$ solution, respectively, and A_s and A_{std} are the absorbances of the unknown sample and aqueous $[Ru(bpy)_3]^{2+}{\cdot}2Cl^-$ solution at excitation wavelengths of 388 nm for $Eu_2(HTH)_6Bpm$ complex and 470 nm for aqueous $[Ru(bpy)_3]^{2+}{\cdot}2Cl^-$ solution, respectively. The η_s and η_{std} terms represent the refractive indices of the corresponding solvents (pure solvents were assumed).

2.2. Synthesis of the $Ln(HTH)_3(H_2O)_2$ complexes (Ln = Eu, Sm, Yb, Er, Pr)

HTH (3 mmol) was dissolved in 15 mL ethanol, and the pH value was adjusted to approximately 8 with appropriate amount of sodium hydroxide solution. After 30 min stirring, $LnCl_3$ (1 mmol) ethanol solution (about 3 mL), prepared separately, was then added dropwise. The solution was refluxed at 70 °C for 1 h, and then cooled to the room temperature. The solvent was removed by evaporation under reduced pressure, and the precipitate obtained was washed with water and diethyl ether three times, respectively, to get the $Ln(HTH)_3(H_2O)_2$ complexes (Ln = Eu, Sm, Yb, Er, Pr).

2.3. Synthesis of the Bpm [38]

Dry DMF (170 mL) was degassed by bubbling argon gas through a frit into the stirred liquid overnight. Triphenylphosphine (9.17 g, 0.035 mol), $NiCl_2$ (1.14 g, 0.0088 mol), and zinc powder (1.14 g, 0.0175 mol) were put under vacuum for 20 min and then added to the solution under argon. Under vigorous stirring at room temperature, the heterogeneous solution turned first red after a few minutes and then gradually brownish. After 1 h, 2-bromopyrimidine (5.56 g, 0.035 mol) was added through a funnel under argon and the solution turned darker. It was stirred vigorously for 1 h at room temperature, heated to 50 °C for 50 h, and filtered through Celite. After being washed with chloroform, the filtrate was evaporated under reduced pressure. The dark green crude solid was suspended in a solution of EDTA (15 g) in aqueous NH_3 (40 mL, 7%). The aqueous layer was extracted with diethyl ether (3 × 30 mL) and subsequently with chloroform (8 × 30 mL). The ether extract contained almost pure triphenylphosphine. The chloroform extract was dried over Na_2SO_4 and evaporated under reduced pressure. The yellow crude product was purified by column chromatography (silica, dichloromethane) and Bpm was recovered as off-white plates: 0.8008 g (yield: 28.9%), M.p.: 110–113 °C (lit. [38] 113–115 °C), ^1H NMR ($CDCl_3$, 500 MHz), δ (ppm) 7.468 (t, 2H, J = 4.5 Hz), 9.053 (s, 4H). IR (KBr) (cm^{-1}) 640, 767 w, 816 w, 985 w, 1144 w, 1401 vs, 1432 w, 1556 s, 2970 w, 3034 w, and 3057 w.

2.4. Synthesis of the $Ln_2(HTH)_6Bpm$ complexes (Ln = Eu, Sm, Er, Yb, Pr)

A solution of $Ln(HTH)_3(H_2O)_2$ (1.0 mmol) and Bpm (0.5 mmol) in 15 mL of acetonitrile were refluxed at 70 °C for 5 h under nitrogen and then cooled to room temperature. The precipitates were collected by filtration and recrystallized from acetonitrile to give the corresponding lanthanide complexes. The yield, melting point (M.p.) and elemental analysis data of all $Ln_2(HTH)_6Bpm$ complexes were listed as follows.

$Eu_2(HTH)_6Bpm$ (21.8%), M.p.: 258–259 °C; Anal. Calcd for $Eu_2(HTH)_6Bpm$ ($Eu_2C_{68}H_{30}N_4O_{12}S_6F_{42}$, 2389.24): C 34.18, H 1.27, N 2.34. Found: C 34.17, H 1.21, N 2.37; $Sm_2(HTH)_6Bpm$ (51.5%), M.p.: 256–258 °C; Anal. Calcd for $Sm_2(HTH)_6Bpm$ ($Sm_2C_{68}H_{30}N_4O_{12}S_6F_{42}$, 2386.03): C 34.23, H 1.27, N 2.35. Found: C 34.21, H 1.20, N 2.33; $Er_2(HTH)_6Bpm$ (52.1%), M.p.: 258–261 °C; Anal. Calcd for $Er_2(HTH)_6Bpm$ ($Er_2C_{68}H_{30}N_4O_{12}S_6F_{42}$, 2419.83): C 33.75, H 1.25, N 2.32. Found: C 33.76, H 1.21, N 2.32; $Pr_2(HTH)_6Bpm$ (20.7%), M.p.: 241–244 °C; Anal. Calcd for $Pr_2(HTH)_6Bpm$ ($Pr_2C_{68}H_{30}N_4O_{12}S_6F_{42}$, 2367.13): C 34.50, H 1.28, N 2.37. Found: C 34.59, H 1.26, N 2.47; $Yb_2(HTH)_6Bpm$ (50.7%), M.p.: 263–264 °C; Anal. Calcd for $Yb_2(HTH)_6Bpm$ ($Yb_2C_{68}H_{30}N_4O_{12}S_6F_{42}$, 2431.39): C 33.59, H 1.24, N 2.30. Found: C 33.51, H 1.21, N 2.27.

3. Results and discussion

3.1. Structural analysis

The crystal structure of $Eu_2(HTH)_6Bpm$ is depicted in Fig. 1, and the crystal data are presented in Table 1; selected bond distances and angles for the complexes are listed in Table 2. The structural analysis of the complex indicates that it crystallizes in the monoclinic space group $P2_1/c$ with the Bpm ligand situated

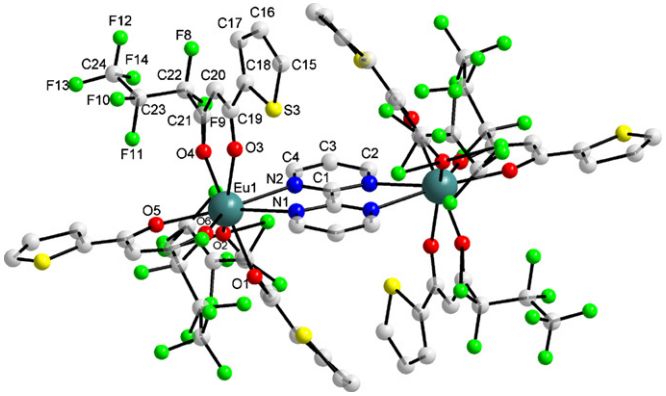

Fig. 1. Molecular structure of $Eu_2(HTH)_6Bpm$ complex showing the atomic numbering scheme, H-atoms are omitted for clarity.

Table 1
Summary of crystal data information and collection/refinement parameters for $Eu_2(HTH)_6Bpm$ complex.

Formula	$C_{68}H_{30}Eu_2F_{42}N_4O_{12}S_6$
FW	2389.24
Cryst. syst.	Monoclinic
Space group	$P2_1/c$
a (Å)	12.125(4)
b (Å)	20.956(7)
c (Å)	16.127(6)
α (°)	90.00
β (°)	104.255(4)
γ (°)	90.00
V (Å^3)	3972(2)
Z	2
ρ_{calcd} (g/cm^3)	1.998
μ (Mo Kα) (mm^{-1})	1.885
F (000) (e)	2324
Cryst. size (mm)	0.16 × 0.15 × 0.14
Reflns collected	19,163
Unique	6991
GOF on F^2	1.040
R_1, wR_2 [$I > 2\sigma(I)$]	0.1081, 0.2519
R_1, wR_2 (all data)	0.2253, 0.2879

about a crystallographic center of symmetry. Each central Eu^{3+} ion is coordinated by six oxygen atoms from three HTH ligands and two nitrogen atoms from Bpm ligand, resulting in a coordination number of eight for each central metal ion. The coordination geometry of the metal can be described as a distorted square antiprism with six oxygen atoms and two nitrogen atoms. The average Eu–O bond length is 2.302 Å and the average Eu–N bond length is 2.600 Å. The intramolecular Eu. . .Eu distance across the bridging Bpm ligand is 6.801(2) Å. The individual Bpm rings are planar, with a mean deviation of 0.008(6) Å for both rings.

Table 2
Selected bond lengths (Å) and angles (°) for $Eu_2(HTH)_6Bpm$ crystal.

Eu(1)–O(1)	2.320(15)	Eu(1)–O(2)	2.330(15)
Eu(1)–O(3)	2.303(14)	Eu(1)–O(4)	2.305(15)
Eu(1)–O(5)	2.264(11)	Eu(1)–O(6)	2.293(12)
Eu(1)–N(1)	2.627(14)	Eu(1)–N(2)	2.572(14)
O(3)–Eu(1)–O(1)	135.7(6)	O(4)–Eu(1)–N(1)	124.8(5)
O(4)–Eu(1)–O(1)	146.6(6)	O(5)–Eu(1)–N(1)	147.2(5)
O(5)–Eu(1)–O(1)	100.2(5)	O(6)–Eu(1)–N(1)	75.6(4)
O(6)–Eu(1)–O(1)	79.0(6)	N(2)–Eu(1)–N(1)	61.8(5)
O(1)–Eu(1)–O(2)	72.2(8)	O(1)–Eu(1)–N(2)	86.4(6)
O(3)–Eu(1)–O(2)	143.5(7)	O(2)–Eu(1)–N(2)	73.3(6)
O(4)–Eu(1)–O(2)	75.2(7)	O(3)–Eu(1)–N(2)	84.3(4)
O(5)–Eu(1)–O(2)	81.6(6)	O(4)–Eu(1)–N(2)	77.8(5)
O(6)–Eu(1)–O(2)	136.1(6)	O(5)–Eu(1)–N(2)	150.7(5)
O(5)–Eu(1)–O(3)	108.7(4)	O(6)–Eu(1)–N(2)	137.4(5)
O(6)–Eu(1)–O(3)	79.2(5)	O(1)–Eu(1)–C(21)	157.3(7)
O(3)–Eu(1)–O(4)	72.1(5)	O(2)–Eu(1)–C(21)	88.3(8)
O(5)–Eu(1)–O(4)	81.5(5)	O(3)–Eu(1)–C(21)	58.2(6)
O(6)–Eu(1)–O(4)	131.6(5)	O(4)–Eu(1)–C(21)	13.9(6)
O(5)–Eu(1)–O(6)	71.8(4)	O(5)–Eu(1)–C(21)	87.9(5)
O(1)–Eu(1)–N(1)	69.3(6)	O(6)–Eu(1)–C(21)	123.8(5)
O(2)–Eu(1)–N(1)	121.3(6)	N(1)–Eu(1)–C(21)	114.0(6)
O(3)–Eu(1)–N(1)	68.2(4)	N(2)–Eu(1)–C(21)	76.7(5)

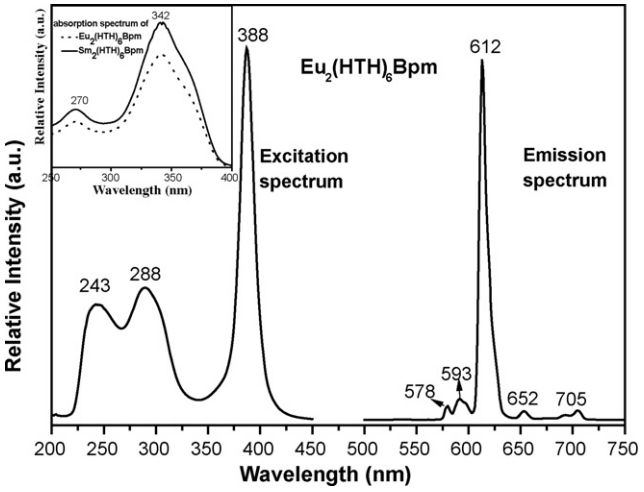

Fig. 2. The excitation and emission spectra of $Eu_2(HTH)_6Bpm$ complex and absorption (inset) spectra of $Eu_2(HTH)_6Bpm$ and $Sm_2(HTH)_6Bpm$ complexes in CH_2Cl_2 solution (1×10^{-3} mol L^{-1}) at room temperature.

3.2. Photoluminescence properties

Because the intraconfigurational f–f transitions are forbidden, absorption of the lanthanide (III) ions is very weak. In most cases, the lanthanide ions are sensitized by organic ligands and exhibit the characteristic luminescence of the corresponding Ln^{3+} ions [39,40]. Upon excitation of the ligand, all the $Ln_2(HTH)_6Bpm$ (Ln = Eu, Sm, Er, Yb, Pr) complexes exhibit one or more spectral emission bands in the visible or near-infrared region. Thus, to provide a clear understanding of the luminescence of this series of lanthanide complexes, the photoluminescence spectra of all complexes were characterized in CH_2Cl_2 solution at room temperature.

The electronic absorption spectra of all complexes were recorded in CH_2Cl_2 solution. They are very similar, both in the shapes and in the intensities, because the absorption of ions is very weak compared to the organic ligands. So, only the absorption spectra of $Eu_2(HTH)_6Bpm$ complex and $Sm_2(HTH)_6Bpm$ complexes are inserted in Fig. 2. There are two peaks at 270 and 342 nm, respectively. The former is attributed to π-π* transition of the Bpm ligand and the electronic transitions of the β-diketonate is peaked at 342 nm.

Fig. 2 also shows the excitation and emission spectra of the $Eu_2(HTH)_6Bpm$ in CH_2Cl_2 solution. It can be found that the excitation spectrum, obtained by monitoring the $^5D_0 \rightarrow {}^7F_2$ transition at 612 nm for $Eu_2(HTH)_6Bpm$, has a wide band peaked at 243 and 288 nm, and a sharp band peaked at 388 nm. Obviously, the excitation spectrum is similar with the absorption one except for the split of the former band. The former band is due to the absorption of the neutral ligand of Bpm and the latter is belonging to the absorption of the ligand of HTH. Excitation of the ligands (388 nm) leads to sharp emission peaks arising from transitions between $^5D_0$–^7F_J components (J = 0, 1, 2, 3, 4). The typical red color of europium emission is mostly attributed to the strongest transition $^5D_0$–$^7F_2$ centered at 612 nm. The emission bands at 578 and 652 nm are very weak because their corresponding transitions $^5D_0 \rightarrow {}^7F_{0,3}$ are forbidden both for magnetic and electric dipole. The intensity of the emission band at 593 nm ($^5D_0 \rightarrow {}^7F_1$) is relatively strong and

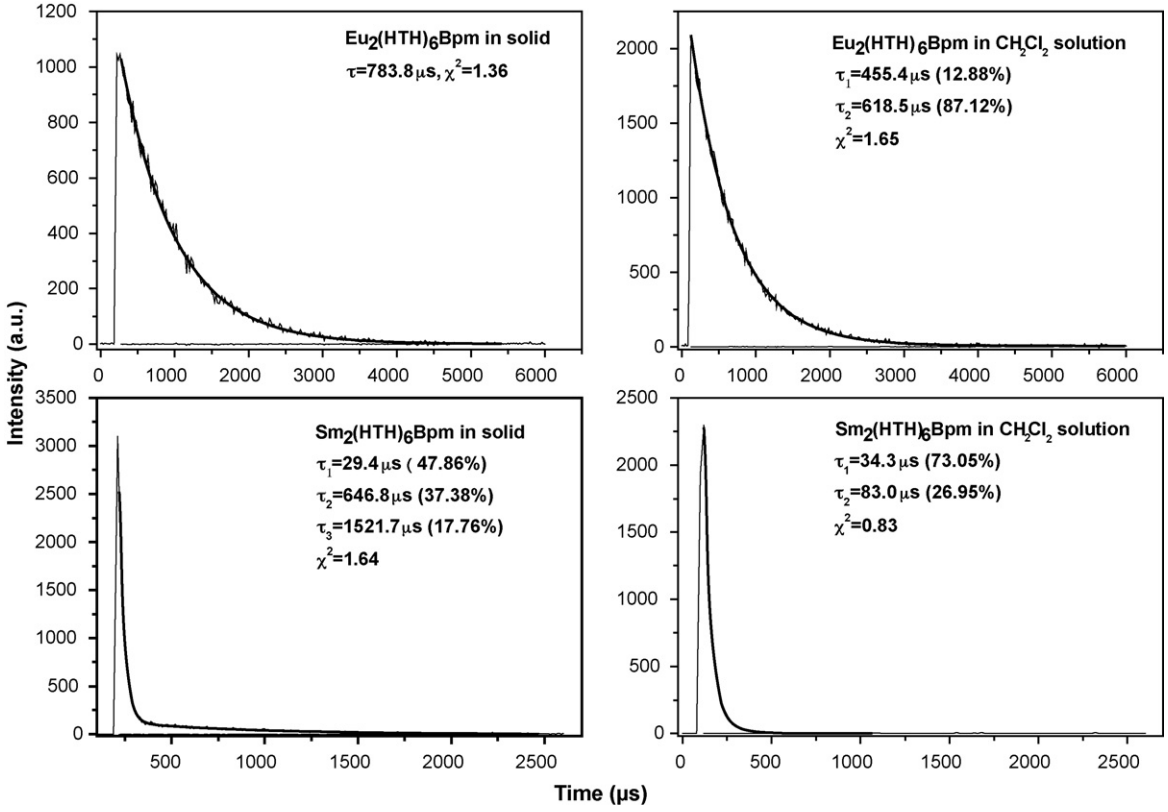

Fig. 3. The emission decay curves of $Eu_2(HTH)_6Bpm$ (up, $^5D_0$, λ_{em} = 612 nm) and $Sm_2(HTH)_6Bpm$ (down, $^4G_{5/2}$, λ_{em} = 648 nm), respectively, both in solid and in CH_2Cl_2 solution at room temperature.

independent on the coordination environment due to its magnetic nature. On the contrary, the $^5D_0 \rightarrow {}^7F_2$ transition is of induced electric dipole character and its corresponding intense emission at ~612 nm is very sensitive to the coordination environment [36]. The emission decay curves of $^5D_0$ level are best fitted by mono-exponential and bi-exponentials in solid and in CH_2Cl_2 solution, respectively (Fig. 3). The emission lifetime of the $Eu_2(HTH)_6Bpm$ complex in the solid state is determined to be 783.8 μs (χ^2 = 1.362). But in CH_2Cl_2 solution the luminescence decay time data of the $Eu_2(HTH)_6Bpm$ complex are τ_{obs} = 618.5 μs (87.12%) and 455.4 μs (12.88%) (χ^2 = 1.652, Fig. 3 and Table 3), a little lower than that in solid state due to the solvent quenching effects. C–H vibrations in the CH_2Cl_2 molecule can provide an efficient non-radiative pathway for the relaxation of the luminescent state of the emitting lanthanide ions by vibronic coupling, since it can be effectively mediated by the ubiquitous molecular vibrations, which probably leads to a shorter lived Ln^{3+} ion excited-state [34]. Suppression of such vibrational excitation in the system requires deuteration of the C–H bonds or replacement of C–H bonds with C–F bonds in the ligand [41]. The photoluminescence lifetime refers to the average time the molecule stays in its excited-state before emitting a photon. In most cases, the emission decay curves of excitation level of lanthanide ions are best fitted by mono-exponential. If a decay is not single exponential then that implies that there are different sites for the ion and that each site has a different lifetime. If you have well defined systems where there may be two or three well defined sites then it is appropriate to use multiple exponentials. However, if there are a range of possible environments (or there is energy trans-

Table 3
Photophysical data for all complexes at room temperature in CH_2Cl_2 solution and solid state.

Complex	Medium	Excitation, λ_{max} (nm)[a]	Emission, λ_{max} (nm)[a,b]	Lifetime, τ (μs)[c]	Efficiency, Φ (%)
$Eu_2(HTH)_6Bpm$	Solid	396	613	783.8 χ^2 = 1.36	15.7[d]
	CH_2Cl_2	388	612	455.4 (12.88%) 618.5 (87.12%) χ^2 = 1.65	12.4[d]28.4[e]
$Sm_2(HTH)_6Bpm$	Solid	396	648	29.4 (47.86%)646.8 (37.38%)1521.7 (17.76%)χ^2 = 1.64	[f]
	CH_2Cl_2	386	649	34.3 (73.05%) 83.0 (26.95%) χ^2 = 0.83	1.4[e]
$Yb_2(HTH)_6Bpm$	CH_2Cl_2	378	976	[f]	[f]
$Er_2(HTH)_6Bpm$	CH_2Cl_2	378	1531	[f]	[f]
$Pr_2(HTH)_6Bpm$	CH_2Cl_2	378	1030	[f]	[f]

[a] Emission maxima from not corrected spectra.
[b] Excited by the highest excitation peak.
[c] $Eu_2(HTH)_6Bpm$: λ_{ex} = 388 nm, λ_{em} = 612 nm; $Sm_2(HTH)_6Bpm$: λ_{ex} = 388 nm, λ_{em} = 649 nm.
[d] Estimated by $\Phi_s = \tau_{obs}/\tau_R$, where τ_{obs} and τ_R are the observed and radiative [36,38] lifetimes, respectively.
[e] Calculated by $\Phi_s = \Phi_{std}(I_s A_{std} \eta_s^2)/(I_{std} A_s \eta_{std}^2)$ using air-equilibrated aqueous $[Ru(bpy)_3]^{2+}\cdot 2Cl^-$ solution as a standard sample (Φ_{std} = 2.8%), the error in this method is estimated to be approximately 10% of the measured value.
[f] Not detected.

fer between sites) then fitting with two or three exponentials is not really suitable. In this case it is better to use a stretched exponential function and state that it is an approximation [42].

Photoluminescent lanthanide complexes generally contain light-absorbing chromophores that serve to photosensitize the lanthanide ion. With Eq. (2) Φ can be calculated using the observed luminescence lifetime τ_{obs} if the radiative lifetime, τ_R, is known [36]. Since consistent and reproducible experimental data for the estimation of τ_R are difficult to obtain, we used $\tau_R = 5.0$ ms for Eu(III) from Stein and Wurzberg [43] to calculate the efficiency of the $Eu_2(HTH)_6Bpm$ complex. Therefore, the quantum efficiency of $Eu_2(HTH)_6Bpm$ complex can be obtained as 15.7% in solid (783.79 μs) and 12.4% in CH_2Cl_2 solution, respectively, by Eq. (2) with the major lifetime (618.48 μs, 87.12%). But using Eq. (3) [37] the luminescence quantum yield of the $Eu_2(HTH)_6Bpm$ complex in CH_2Cl_2 solution can be obtained as 28.4% with a standard sample (air-equilibrated aqueous $[Ru(bpy)_3]^{2+}\cdot 2Cl^-$ solution, $\Phi_{std} = 2.8\%$) which near the well known europium complexes such as $Eu(TTA)_3Phen$ ($\Phi_s = 30\%$ [44]), TTA = thenoyltrifluoroacetone, Phen = 1,10-phenanthroline or $Eu(DBM)_3Phen$ ($\Phi_s = 23\%$ [5], DBM = dibenzoylmethane) suggesting it is a potential luminescent material. The experimental value is higher than the data obtained above with the first method because τ_R is not a constant in most cases [36].

Fig. 4 shows the excitation and emission spectra of $Sm_2(HTH)_6Bpm$ complex in CH_2Cl_2 solution. The excitation spectrum, obtained by monitoring the $^4G_{5/2} \rightarrow {}^6H_{9/2}$ transition at 644 nm, is very similar to that of $Eu_2(HTH)_6Bpm$ complex in CH_2Cl_2 solution due to the same ligands in the two compounds. The emission spectrum consists of a series of characteristic emission peaks of Sm^{3+} ion, such as $^4G_{5/2} \rightarrow {}^6H_{5/2}$ (565 nm), $^4G_{5/2} \rightarrow {}^6H_{7/2}$ (611 nm), $^4G_{5/2} \rightarrow {}^6H_{9/2}$ (649 nm) and $^4G_{5/2} \rightarrow {}^6H_{11/2}$ (705 nm). The intensity (I) sequence of the peaks is $I(^4G_{5/2} \rightarrow {}^6H_{9/2}) > I(^4G_{5/2} \rightarrow {}^6H_{7/2}) > I(^4G_{5/2} \rightarrow {}^6H_{5/2}) > I(^4G_{5/2} \rightarrow {}^6H_{11/2})$. The emission decay curves of $^4G_{5/2}$ level are best fitted by multi-exponentials both in solid and in CH_2Cl_2 solution, the corresponding lifetime data are collected in Table 3. From the data we can find that in the CH_2Cl_2 solution the lifetime can be decreased greatly due to the effects the solvent [34].

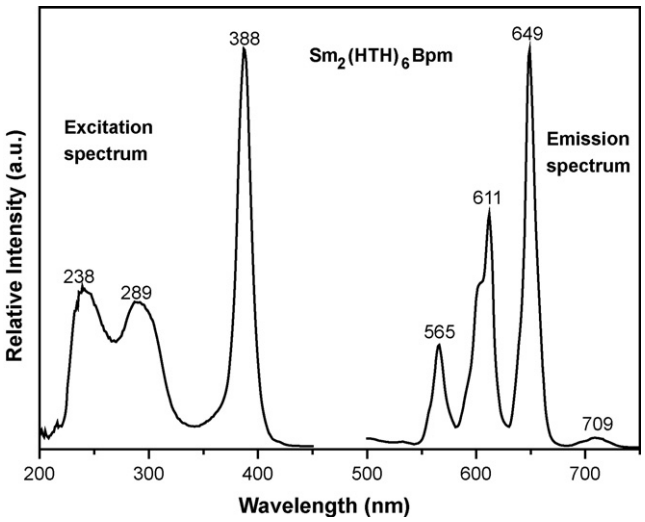

Fig. 4. Excitation and emission spectra of $Sm_2(HTH)_6Bpm$ complex in CH_2Cl_2 solution (1×10^{-3} mol L^{-1}) at room temperature.

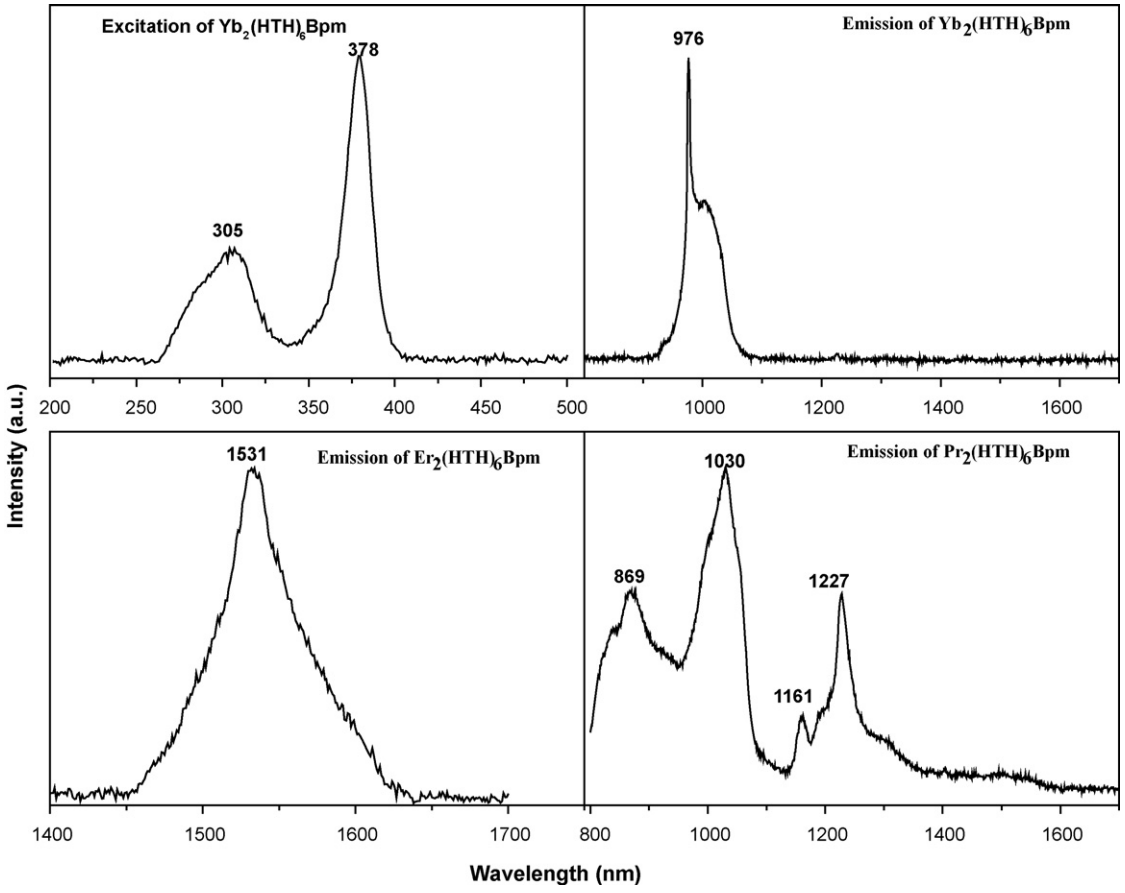

Fig. 5. Excitation and emission spectra of $Ln_2(HTH)_6Bpm$ (Ln = Yb, Er and Pr) complex in CH_2Cl_2 solution at room temperature.

The excitation and emission spectra in NIR region of the $Yb_2(HTH)_6Bpm$, $Er_2(HTH)_6Bpm$ and $Pr_2(HTH)_6Bpm$ complexes are shown in Fig. 5. For the excitation spectrum of the $Yb_2(HTH)_6Bpm$ complex there are only two peaks at 305 and 378 nm, respectively. After ligand-mediated excitation at 378 nm, the $Yb_2(HTH)_6Bpm$ complex emits in the range of 920–1100 nm, with a sharp band at 976 nm assigned to the $^2F_{5/2} \rightarrow {}^2F_{7/2}$ transition of the Yb^{3+} ion and a broader vibronic component at longer wavelength [45]. The Yb^{3+} ion plays an important role in laser emission because of its very simple f–f energy level structure: besides the $^2F_{7/2}$ ground multiplet, there is only the $^2F_{5/2}$ excited multiplet at around 10,000 cm^{-1}. There is no excited-state absorption on reducing the effective laser cross-section, no up-conversion, no concentration quenching, and no absorption in the visible range. The intense Yb^{3+} ion absorption lines are well suited for this range and the smaller Stokes shift (about 650 cm^{-1}) between absorption and emission reduces the thermal loading of the material during laser operation. These properties of the Yb^{3+} ion and the obtained high intensity emission make these Yb complexes very important for various photonic applications in laser diode pumping [46], ionic crystals, glasses [47] and bioprobes [26,48,49].

For the $Er_2(HTH)_6Bpm$ complex, the emission bands centered at 1531 nm cover large spectral range extending from 1450 to 1640 nm, which are attributed to the typical $^4I_{13/2} \rightarrow {}^4I_{15/2}$ transition of the Er^{3+} ion. While emission from a number of excited-states of the Er^{3+} ion is feasible, only emission from the $^4I_{13/2}$ state is observed, which suggests that an efficient non-radiative decay mechanism exists from these states to the $^4I_{15/2}$ state. Erbium-doped materials have been the subject of much interest for many years because the transition around 1530 nm is in the right position of the third telecommunication window. To enable a wide-gain bandwidth for optical amplification, a broad emission band is desirable [50]. The full widths at half maximum (FWHM) of the $^4I_{13/2} \rightarrow {}^4I_{15/2}$ transition for the $Er_2(HTH)_6Bpm$ complex are 58 nm, which enable a wide-gain bandwidth for optical amplification [51].

The NIR emission spectra of $Pr_2(HTH)_6Bpm$ complex consists of four bands at 869, 1030, 1161 and 1227 nm, which can be attributed to $^1D_2 \rightarrow {}^3F_2$, $^1D_2 \rightarrow {}^3F_4$ and $^1G_4 \rightarrow {}^3H_4$ transitions of Pr^{3+} ion, respectively. The luminescent spectra of Pr^{3+} ion are more complicated compared to other lanthanide ions, since the Pr^{3+} ion can show emissions from three different levels ($^3P_0$, $^1D_2$ and $^1G_4$) upon excitation of the organic ligands [52]. Radiative transitions from the $^1D_2$ level are more probable than transitions from the $^3P_0$ level, as radiative transitions are more likely to occur when energy gaps are larger [53]. The $^1D_2$ level exhibits the largest energy gap (6950 cm^{-1}, compared to 3860 cm^{-1} for $^3P_0 \rightarrow {}^1D_2$) to the next lower lying level $^1G_4$. The design of efficient NIR-luminescence materials based on lanthanide complexes remains an area of active investigation. Most researches have been focused on sensitizers with a triplet state matching the receiving lanthanide ion energy level such that efficient energy transfer can be obtained. From our former study [33,34], the triplet state for the HTH ligand is 20,400 cm^{-1}, which is close to the $^3P_0$ level (20,700 cm^{-1}) of Pr^{3+} ion. This small energy gap then would permit energy back-transfer, $^3P_0 \rightarrow L_T$ (where L_T is the triplet ligand state). As a result, the $^3P_0$-luminescence of the Pr^{3+} ion is almost completely quenched by the energy back-transfer upon excitation of the ligands absorption [52].

3.3. Thermal analysis

In order to investigate the stability characteristics of the $Ln_2(HTH)_6Bpm$ (Ln = Eu, Sm, Yb, Er, Pr) complexes, TGA was performed on it in a N_2 atmosphere, and the traces of all complexes are presented in Fig. 6. For all the complexes, thermal decomposition is via a single distinctive stage. The weight loss of complex $Eu_2(HTH)_6Bpm$ started at 301 °C and was completed at 378 °C with an overall weight loss of 58.1%. Complexes $Sm_2(HTH)_6Bpm$, $Yb_2(HTH)_6Bpm$, $Er_2(HTH)_6Bpm$ and $Pr_2(HTH)_6Bpm$ show the similar thermal characteristics as $Eu_2(HTH)_6Bpm$ in a N_2 atmosphere: the weight loss of them started at 323 °C, 328 °C, 332 °C and 245 °C and were completed at 389 °C, 393 °C, 396 °C and 369 °C, with an overall weight loss of 68.9%, 69.4%, 69.9% and 67.5%, respectively.

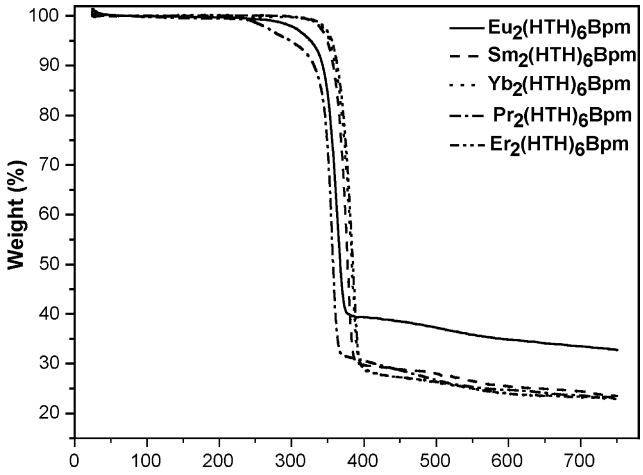

Fig. 6. TGA traces of $Ln_2(HTH)_6Bpm$ (Ln = Eu, Sm, Yb, Er and Pr) complexes.

3.4. Supplementary data

CCDC 734,363 contains the supplementary crystallographic data for $Eu_2C_{68}H_{30}N_4O_{12}S_6F_{42}$. These data can be obtained free of charge from the Cambridge Crystallographic Data Centre, 12 Union Road, Cambridge CB2 1EZ, UK; fax: (+44) 1223 336 033; or e-mail: deposit@ccdc.cam.ac.uk.

4. Conclusions

Based on a bridging ligand Bpm and a sensitizing ligand HTH, five homodinuclear complexes with formula $[Ln_2(HTH)_6Bpm]$ (Ln = Eu, Sm, Er, Yb, Pr) have been synthesized. We have demonstrated that the characteristic luminescence of the corresponding lanthanide complexes upon excitation of the ligand absorption bands. The $Eu_2(HTH)_6Bpm$ complex shows long photoluminescence lifetime and high quantum efficiency. The development of new materials based on binuclear Ln(III) complexes for applications in the field of organic light-emitting diodes (OLEDs), optical amplification, laser systems or medical diagnostics needs further research.

Acknowledgments

We thank the National Natural Science Foundation of China (20701019, 20971067 and 20721002), the Natural Science Foundation of Jiangsu Province (BK2008257), the National Basic Research Program of China (2007CB925103), the Major State Basic Research Development Program (2006CB806104) and the Research Fund for the Doctoral Program of Higher Education (20070284053) for financial support.

References

[1] J. Kido, Y. Okamoto, Organo lanthanide metal complexes for electroluminescent materials, Chem. Rev. 102 (2002) 2357–2368 (and references cited therein).
[2] M. Montalti, L. Prodi, N. Zaccheroni, L. Charbonniere, L. Douce, R. Ziessel, A luminescent anion sensor based on a europium hybrid complex, J. Am. Chem. Soc. 123 (2001) 12694–12695.
[3] K. Binnemans, C. Görller-Walrand, Lanthanide-containing liquid crystals and surfactants, Chem. Rev. 102 (2002) 2303–2346 (and references cited therein).

[4] K. Kuriki, Y. Koike, Y. Okamoto, Plastic optical fiber lasers and amplifiers containing lanthanide complexes, Chem. Rev. 102 (2002) 2347–2356 (and references cited therein).
[5] M.D. McGehee, T. Bergstedt, C. Zhang, A.P. Saab, M.B. O'Regem, G.C. Bazan, V.I. Srdanov, A.J. Heeger, Narrow bandwidth luminescence from blends with energy transfer from semiconducting conjugated polymers to europium complexes, Adv. Mater. 11 (1999) 1349–1354.
[6] G. Yu, Y. Liu, X. Wu, D. Zhu, H. Li, L. Jin, M. Wang, Soluble europium complexes for light-emitting diodes, Chem. Mater. 12 (2000) 2537–2541.
[7] M. Sun, H. Xin, K.-Z. Wang, Y.-A. Zhang, L.-P. Jin, C.-H. Huang, Bright and monochromic red light-emitting electroluminescence devices based on a new multifunctional europium ternary complex, Chem. Commun. (2003) 702–703.
[8] F. Liang, Q. Zhou, Y. Cheng, L. Wang, D. Ma, X. Jing, F. Wang, Oxadiazole-functionalized europium(III) β-diketonate complex for efficient red electroluminescence, Chem. Mater. 15 (2003) 1935–1937.
[9] P.-P. Sun, J.-P. Duan, H.-T. Shih, C.-H. Cheng, Europium complex as a highly efficient red emitter in electroluminescent devices, Appl. Phys. Lett. 81 (2002) 792–794.
[10] Y. Kawamura, Y. Wada, Y. Hasegawa, M. Iwamuro, T. Kitamura, S. Yanagida, Observation of neodymium electroluminescence, Appl. Phys. Lett. 74 (1999) 3245–3247.
[11] S.I. Klink, G.A. Hebbink, L. Grave, F.C.J.M. Van Veggel, D.N. Reinhoudt, L.H. Sloott, A. Polman, J.W. Hoftraat, Sensitized near-infrared luminescence from polydentate triphenylene-functionalized Nd3+, Yb3+, and Er3+ complexes, J. Appl. Phys. 86 (1999) 1181–1185.
[12] L.H. Slooff, A. Polman, F. Cacialli, R.H. Friend, G.A. Hebbink, F.C.J.M. Van Veggel, D.N. Reinboudt, Near-infrared electroluminescence of polymer light-emitting diodes doped with a lissamine-sensitized Nd3+ complex, Appl. Phys. Lett. 78 (2001) 2122–2124.
[13] W.P. Gillin, R.J. Curry, Erbium (III) tris(8-hydroxyquinoline) (ErQ): a potential material for silicon compatible 1.5 μm emitters, Appl. Phys. Lett. 74 (1999) 798–800.
[14] B.S. Harrison, T.J. Foley, M. Bouguettaya, J.M. Boncells, J.R. Reynolds, K.S. Schanze, J. Shim, P.H. Holloway, G. Padmanaban, J.R. Krishnan, Near-infrared electroluminescence from conjugated polymer/lanthanide porphyrin blends, Appl. Phys. Lett. 79 (2001) 3770–3772.
[15] R.Y. Wang, D. Song, C. Seward, Y. Tao, S.N. Wang, Syntheses, structures, and electroluminescence of Ln_2(acac-azain)$_4$(μ-acac-azain)$_2$ [acac-azain = 1-(N-7-azaindolyl)-1,3-butanedionato, Ln = Tb(III) and Y(III)], Inorg. Chem. 41 (2002) 5187–5192.
[16] W.-Y. Yang, L. Chen, S.N. Wang, Syntheses, structures, and luminescence of novel lanthanide complexes of tripyridylamine, N,N,N′,N′-tetra(2-pyridyl)-1,4-phenylenediamine and N,N,N′,N′-tetra(2-pyridyl)biphenyl-4,4′-diamine, Inorg. Chem. 40 (2001) 507–515.
[17] H.S. Jang, C.-H. Shin, B.-J. Jung, D.-H. Kim, H.-K. Shim, Y.K. Do, Synthesis and characterization of dinuclear europium complexes showing pure red electroluminescence, Eur. J. Inorg. Chem. (2006) 718–725.
[18] S.V. Eliseeva, M. Ryazanov, F. Gumy, S.I. Troyanov, L.S. Lepnev, J.-C.G. Bünzli, N.P. Kuzmina, Dimeric complexes of lanthanide(III) hexafluoroacetylacetonates with 4-cyanopyridine N-oxide: synthesis, crystal structure, magnetic and photoluminescent properties, Eur. J. Inorg. Chem. (2006) 4809–4820.
[19] S.V. Eliseeva, O.V. Kotova, F. Gumy, S.N. Semenov, V.G. Kessler, L.S. Lepnev, J.-C.G. Bünzli, N.P. Kuzmina, Role of the ancillary ligand N,N-dimethylaminoethanol in the sensitization of EuIII and TbIII luminescence in dimeric β-diketonates, J. Phys. Chem. A 112 (16) (2008) 3614–3626.
[20] J. Legendziewicz, J. Cybinska, L.C. Thompson, L. Pan, W. Brennessel, Structure and photophysics of a europium dimeric system, Eu_2(HFAA)$_2$(Dipy)$_2$(TFOAc)$_2$(OAc)$_2$, in the solid state and solution, J. Alloys Compd. 451 (2008) 88–93.
[21] D. D'Cunha, D. Collins, G. Richards, G.S. Vincent, S. Swavey, Dinuclear lanthanide(III) complexes containing β-diketonate terminal ligands bridged by 2,2′-bipyrimidine, Inorg. Chem. Commun. 9 (2006) 979–984.
[22] R. Sultan, K. Gadamsetti, S. Swavey, Synthesis electrochemistry and spectroscopy of lanthanide(III) homodinuclear complexes bridged by polyazine ligands, Inorg. Chim. Acta 359 (2006) 1233–1238.
[23] A. Fratinia, S. Swavey, Luminescent and structural properties of a Eu(III) complex: formation of a one-dimensional array bridged by 2,2′-bipyrimidine, Inorg. Chem. Commun. 10 (2007) 636–638.
[24] S. Klink, P. Alink, L. Grave, F. Peters, J. Hofstraat, F. Geurts, F. Van Veggel, Fluorescent dyes as efficient photosensitizers for near-infrared Nd^{3+} emission, J. Chem. Soc. Perkin Trans. 2 (2001) 363–372.
[25] S. Quici, M. Cavazzini, G. Marzanni, G. Accorsi, N. Armaroli, B. Ventura, F. Barigelletti, Visible and near-infrared intense luminescence from water-soluble lanthanide [Tb(III), Eu(III), Sm(III), Dy(III), Pr(III), Ho(III), Yb(III), Nd(III), Er(III)] complexes, Inorg. Chem. 44 (2005) 529–537.
[26] G.M. Davies, R.J. Aarons, G.R. Motson, J.C. Jeffery, H. Adams, S. Faulkner, M.D. Ward, Structural and near-IR photophysical studies on ternary lanthanide complexes containing poly(pyrazolyl)borate and 1,3-diketonate ligands, J. Chem. Soc. Daltons Trans. (2004) 1136–1144.
[27] L.N. Sun, H.J. Zhang, Q.G. Meng, F.Y. Liu, L.S. Fu, C.Y. Peng, J.B. Yu, G.L. Zheng, S.B. Wang, Near-infrared luminescent hybrid materials doped with lanthanide (Ln) complexes (Ln = Nd, Yb) and their possible laser application, J. Phys. Chem. B 109 (2005) 6174–6182.
[28] T.J. Foley, B.S. Harrison, A.S. Knefely, K.A. Abboud, J.R. Reynolds, K.S. Schanze, J.M. Boncella, Facile preparation and photophysics of near-infrared luminescent lanthanide(III) monoporphyrinate complexes, Inorg. Chem. 42 (2003) 5023–5032.
[29] M.P.O. Wolbers, F.C.J.M. van Veggel, B.H.M. Snellink-Ruël, J.W. Hofstraat, F.A.J. Geurts, D.N. Reinhoudt, Photophysical studies of m-terphenyl-sensitized visible and near-infrared emission from organic 1:1 lanthanide ion complexes in methanol solutions, J. Chem. Soc., Perkin Trans. 2 (1998) 2141–2150.
[30] F.X. Zang, W.L. Li, Z.R. Hong, H.Z. Wei, M.T. Li, X.Y. Sun, C.S. Lee, Observation of 1.5 μm photoluminescence and electroluminescence from a holmium organic complex, Appl. Phys. Lett. 84 (2004) 5115–5117.
[31] R.A. Pavinato, J.A. Walk, M.E. McGuire, Spectroscopic and electrochemical characterization of the asymmetric bimetallic ruthenium(II) complex [(bpy)$_2$$Ru^{II}$(bpym)$Ru^{II}$(NH$_3$)$_4$](PF$_6$)$_4$·3H$_2$O, Inorg. Chem. 32 (1993) 4982–4984.
[32] S. Swavey, Z. Fang, K.J. Brewer, Mixed-metal supramolecular complexes coupling phosphine-containing Ru(II) light absorbers to a reactive Pt(II) through polyazine bridging ligands, Inorg. Chem. 41 (2002) 2598–2607.
[33] Y.X. Zheng, L.S. Fu, Y.H. Zhou, J.B. Yu, Y.N. Yu, S.B. Wang, H.J. Zhang, Electroluminescence based on a β-diketonate ternary samarium complex, J. Mater. Chem. 12 (2002) 919–923.
[34] L.N. Sun, J.B. Yu, G.L. Zheng, H.J. Zhang, Q.G. Meng, C.Y. Peng, L.S. Fu, F.Y. Liu, Y.N. Yu, Syntheses, structures and near-IR luminescent studies on ternary lanthanide (Er^{III}, Ho^{III}, Yb^{III}, Nd^{III}) complexes containing 4,4,5,5,6,6,6-heptafluoro-1-(2-thienyl)hexane-1,3-dionate, Eur. J. Inorg. Chem. (2006) 3962–3973.
[35] J.W. Verhoeven, Glossary of terms used in photochemistry, Pure Appl. Chem. 68 (1996) 2223–2286.
[36] M.H.V. Werts, R.T.F. Jukes, J.W. Verhoeven, The emission spectrum and the radiative lifetime of Eu^{3+} in luminescent lanthanide complexes, Phys. Chem. Phys. 4 (2002) 1542–1548.
[37] D.P. Rillema, D.G. Taghdiri, D.S. Jones, C.D. Keller, L.A. Worl, T.J. Meyer, H.A. Levy, Structure and redox and photophysical properties of a series of ruthenium heterocycles based on the ligand 2,3-bis(2-pyridyl)quinoxaline, Inorg. Chem. 26 (1987) 578–585.
[38] P.F.H. Schwab, F. Fleischer, J. Michl, Preparation of 5-brominated and 5,5′-dibrominated 2,2′-bipyridines and 2,2′-bipyrimidines, J. Org. Chem. 67 (2002) 443–449.
[39] J. Thompson, R.I.R. Blyth, G. Gigli, R. Cingolani, Obtaining characteristic 4f–4f luminescence from rare earth organic chelates, Adv. Funct. Mater. 14 (2004) 979–984.
[40] S.I. Klink, L. Grave, D.N. Reinhoudt, F.C.J.M. van Veggel, M.H.V. Werts, F.A.J. Geurts, J.W. Hofstraat, A systematic study of the photophysical processes in polydentate triphenylene-functionalized Eu^{3+}, Tb^{3+}, Yb^{3+}, and Er^{3+} complexes, J. Phys. Chem. A 104 (2000) 5457–5468.
[41] S. Yanagida, Y. Hasegawa, K. Murakoshi, Y. Wada, N. Nakashima, T. Yamanaka, Strategies for enhancing photoluminescence of Nd^{3+} in liquid media, Coord. Chem. Rev. 171 (1998) 461–480.
[42] R.H.C. Tan, J.M. Pearson, Y. Zheng, P.B. Wyatt, W.P. Gillin, Evidence for erbium–erbium energy migration in erbium (III) bis(perfluoro-p-tolyl)phosphinate, Appl. Phys. Lett. 92 (2008) 103303–103305.
[43] G. Stein, E. Wurzberg, Energy gap law in the solvent isotope effect on radiationless transitions of rare earth ions, J. Chem. Phys. 62 (1975) 208–213.
[44] C. Adachi, M.A. Baldo, S.R. Forrest, Electroluminescence mechanisms in organic light emitting devices employing a europium chelate doped in a wide energy gap bipolar conducting host, J. Appl. Phys. 87 (2000) 8049–8055.
[45] P. Lenaerts, K. Driesen, R. Van Deun, K. Binnemans, Covalent coupling of luminescent tris(2-thenoyltrifluoroacetonato)lanthanide(III) complexes on a merrifield resin, Chem. Mater. 17 (2005) 2148–2154.
[46] G. Boulon, A. Collombet, A. Brenier, M.T. Cohen-Adad, A. Yoshikawa, K. Lebbou, J.H. Lee, T. Fukuda, Structural and spectroscopic characterization of nominal Yb^{3+}:$Ca_8La_2(PO_4)_6O_2$ oxyapatite single crystal fibers grown by the micro-pulling-down method, Adv. Funct. Mater. 11 (2001) 263–270.
[47] C. Reinhard, H.U. Güdel, High-resolution optical spectroscopy of Na_3[Ln(dpa)$_3$]·13H$_2$O with Ln = Er^{3+}, Tm^{3+}, Yb^{3+}, Inorg. Chem. 41 (2002) 1048–1055.
[48] C.L. Maupin, R.S. Dickins, L.G. Govenlock, C.E. Mathieu, D. Parker, J.A.G. Williams, J.P. Riehl, The measurement of circular polarization in the near-IR luminescence from chiral complexes of Yb(III) and Nd(III), J. Phys. Chem. A 104 (2000) 6709–6717.
[49] M.H.V. Werts, R.H. Woudenberg, P.G. Emmerink, R.V. Gassel, J.W. Hofstraat, J.W. Verhoeven, A near-infrared luminescent label based on Yb^{III} ions and its application in a fluoroimmunoassay, Angew. Chem. Int. Ed. 39 (2000) 4542–4544.
[50] R.V. Deun, P. Nockemann, C. Görller-Walrand, K. Binnemans, Strong erbium luminescence in the near-infrared telecommunication window, Chem. Phys. Lett. 397 (2004) 447–450.
[51] O.H. Park, S.Y. Seo, B.S. Bae, J.H. Shin, Indirect excitation of Er^{3+} in sol–gel hybrid films doped with an erbium complex, Appl. Phys. Lett. 82 (2003) 2787–2789.
[52] A.I. Voloshin, N.M. Shavaleev, V.P. Kazakov, Luminescence of praseodymium(III) chelates from two excited states ($^3P_0$ and $^1D_2$) and its dependence on ligand triplet state energy, J. Lumin. 93 (2001) 199–204.
[53] A. Babai, A.V. Mudring, Anhydrous praseodymium salts in the ionic liquid [bmpyr][Tf_2N]: structural and optical properties of [bmpyr]$_4$[PrI_6][Tf_2N] and [bmyr]$_2$[Pr(Tf_2N)$_5$], Chem. Mater. 17 (2005) 6230–6238.